

Coexistence of superconductivity and ferromagnetism in $\text{Sr}_{0.5}\text{Ce}_{0.5}\text{FBiS}_2$

Lin Li,¹ Yuke Li,^{1,*} Yuefeng Jin,¹ Haoran Huang,¹ Bin Chen,¹ Xiaofeng Xu,¹ Jianhui Dai,¹ Li Zhang,² Xiaojun Yang,³ Huifei Zhai,³ Guanghan Cao,³ and Zhuan Xu³

¹*Department of Physics, Hangzhou Normal University, Hangzhou 310036, China*

²*Department of Physics, China Jiliang University, Hangzhou 310018, China*

³*State Key Lab of Silicon Materials and Department of Physics, Zhejiang University, Hangzhou 310027, China*

(Received 20 July 2014; revised manuscript received 8 January 2015; published 20 January 2015)

Through the combination of x-ray diffraction, electrical transport, magnetic susceptibility, and heat capacity measurements, we studied the effect of Ce doping in the newly discovered SrFBiS_2 system. It is found that $\text{Sr}_{0.5}\text{Ce}_{0.5}\text{FBiS}_2$ undergoes a second-order transition below ~ 7.5 K, followed by a superconducting transition with the critical temperature $T_c \sim 2.8$ K. Our transport, specific heat, and dc-magnetization results suggest the presence of bulk ferromagnetic correlation of Ce ions below 7.5 K that coexist with superconductivity when the temperature is further lowered below 2.8 K.

DOI: [10.1103/PhysRevB.91.014508](https://doi.org/10.1103/PhysRevB.91.014508)

PACS number(s): 74.70.Xa, 74.25.Dw, 75.50.Lk

I. INTRODUCTION

The fascinating relationship between superconductivity (SC) and magnetic ordering has been a central issue in condensed matter physics for several decades. It has been generally believed that, within the context of the Bardeen–Cooper–Schrieffer (BCS) theory, the conduction electrons cannot be ordered magnetically and superconducting simultaneously [1]. In other words, superconductivity and magnetism are two antagonistic phenomena. Even though the superconducting pairing in cuprates, heavy fermions, and Fe-based superconductors is mediated by antiferromagnetic spin fluctuations [2,3], SC can be generally induced by suppressing the magnetic ordering with chemical doping or pressure [4,5]. Accordingly, the evidence for the coexistence of superconductivity and ferromagnetism (FM) in the same system is very rare and has only been claimed in a few compounds (UGe_2 , URhGe , EuFe_2 , $\text{As}_{2-x}\text{P}_x$) [6–9].

Recently, superconductivity with a transition temperature T_c of 8.6 K in a novel BiS_2 -based superconductor $\text{Bi}_4\text{O}_4\text{S}_3$ has been discovered [10]. Immediately after this finding, several other BiS_2 -based superconductors, $\text{LnO}_{1-x}\text{F}_x\text{BiS}_2$ ($\text{Ln} = \text{La}, \text{Ce}, \text{Pr}, \text{Nd}$) [11–15] with the highest T_c of 10 K have been intensively studied. In analogy to cuprates and iron-based superconductors, the BiS_2 -based compounds also possess a layered crystal structure consisting of superconducting BiS_2 layers intercalated with various block layers, e.g., $\text{Bi}_4\text{O}_4(\text{SO}_4)_{1-x}$ or $[\text{Ln}_2\text{O}_2]^{2-}$. Apparently, the common BiS_2 layer is believed to be the key structural element in search for a new superconductor, where superconductivity can be induced by chemical doping into the intercalated block layers. Indeed, through the replacement of the LaO layer by the SrF block, a new BiS_2 -based superconductor $\text{Sr}_{1-x}\text{La}_x\text{FBiS}_2$, which is isostructural to LaOBiS_2 , has been successfully synthesized and studied [16–18]. The parent compound SrFBiS_2 shows semiconducting-like behavior, and the substitution of La into the Sr site can induce a T_c as high as 2.8 K.

Up to now, most studies on LnOBiS_2 -based systems have focused on their electronic structure [19], superconducting

transition temperature [20], and the pairing symmetry [21–23]. Although most experimental studies [24–26] and theoretical calculations [21,22] seem to support the conventional s -wave pairing in these systems, the coexistence of superconductivity and ferromagnetism was recently proposed for the $\text{CeO}_{1-x}\text{F}_x\text{BiS}_2$ superconductor [14,27], which is apparently beyond the conventional BCS framework. In this paper, we demonstrate another example where the superconductivity is in close proximity to the ferromagnetism. We report a successful synthesis of Ce-doped $\text{Sr}_{0.5}\text{Ce}_{0.5}\text{FBiS}_2$ superconductor, in which the diluted Ce ions order ferromagnetically at 7.5 K, and the system becomes superconducting below ~ 3 K.

II. EXPERIMENTAL

The polycrystalline sample $\text{Sr}_{0.5}\text{Ce}_{0.5}\text{FBiS}_2$ was synthesized by a two-step solid-state reaction method. The starting materials were high purity ($\geq 99.9\%$) Ce_2S_3 , SrF_2 , CeF_3 , Bi_2S_3 , and S powders and were weighted according to their stoichiometric ratio and then fully ground in an agate mortar. The mixture of powder was then pressed into pellets, heated in an evacuated quartz tube at 1073 K for 24 h, and finally quenched to room temperature. In order to get the pure and homogeneous phase, the sample was annealed at 973 K for 10 h again. Crystal-structure characterization was performed by powder x-ray diffraction (XRD) at room temperature using a D/Max-rA diffractometer with $\text{Cu } K\alpha$ radiation and a graphite monochromator. The XRD data were collected in a step-scan mode for $10^\circ \leq 2\theta \leq 120^\circ$. Lattice parameters were obtained by Rietveld refinements. The electrical resistivity was measured with a standard four-terminal method covering the temperature range from 0.4 to 300 K in a commercial Quantum Design PPMS-9 system with a ^3He refrigeration insert. The measurements of specific heat were also performed in this system. dc magnetic properties were measured on a Quantum Design Magnetic Property Measurement System (MPMS-7).

III. RESULTS AND DISCUSSION

Figure 1 shows the powder XRD patterns of the $\text{Sr}_{0.5}\text{Ce}_{0.5}\text{FBiS}_2$ sample at room temperature, as well as the result of the Rietveld structural refinement. Overall, the main

*yklee@hznu.edu.cn

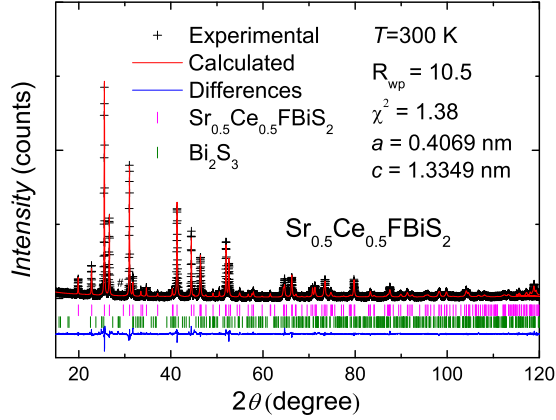


FIG. 1. (Color online) Powder x-ray diffraction patterns and the Rietveld refinement profile for $\text{Sr}_{0.5}\text{Ce}_{0.5}\text{FBiS}_2$ samples at room temperature. The # peak positions designate the impurity phase of Bi_2S_3 .

diffraction peaks of this sample can be well indexed based on a tetragonal cell structure with the $P4/nmm$ space group. In addition to the principal phase, extra minor peaks arising from the impurity phase of Bi_2S_3 with $Pnma$ symmetry can also be observed [28], and its content is estimated by Rietveld refinement to be about 6%. The refined lattice parameters are extracted to be $a = 4.0695 \text{ \AA}$ and $c = 13.3491 \text{ \AA}$, which are shortened by 0.32% and 3.3%, respectively, compared with those of the parent compound SrFBiS_2 [16]. As a result, the cell volume shrinks by 3.9% for $\text{Sr}_{0.5}\text{Ce}_{0.5}\text{FBiS}_2$. This result suggests that Ce ions were partially substituted to Sr ones.

Figure 2(a) shows the temperature dependence of electrical resistivity ρ under zero field and 9 T for the $\text{Sr}_{0.5}\text{Ce}_{0.5}\text{FBiS}_2$ sample. Its zero-field resistivity increases monotonically with decreasing temperature but its value drops by several orders of magnitude compared to the undoped sample [16]. Meanwhile, it also shows thermally activated behavior with decreasing temperature from 300 K. By using the thermal activation formula $\rho(T) = \rho_0 \exp(E_a/k_B T)$ to fit $\rho(T)$ at the temperature range from 120 to 300 K, we obtain the thermal activation energy E_a of $\sim 22.1 \text{ meV}$, which is far smaller than that of the undoped SrFBiS_2 sample (38.2 meV) [16,17], suggesting the decrease of gap size due to electron doping. With further cooling, a sharp superconducting transition with $T_c = 2.8 \text{ K}$, developing from a semiconducting-like normal state, is clearly observed. This feature is commonly observed in BiS_2 -based superconductors [11–15]. As the magnetic field H increases to 9 T, superconductivity is completely suppressed. The normal state recovered by the magnetic field is semiconducting like down to 0.5 K. On closer examination, as shown in the lower inset of Fig. 2(a), the negative magnetoresistance can be clearly observed below 7.5 K and reaches $\sim -8\%$ at 3 K, which will be discussed further below. Similar behavior are also observed in the FM superconductors $\text{EuFe}_2\text{As}_{2-x}\text{P}_x$ [8] and $\text{CeO}_{0.95}\text{F}_{0.05}\text{FeAs}_{1-x}\text{P}_x$ [9]. As a comparison, no significant magnetoresistance was found in the parent compound SrFBiS_2 [17] and $\text{Sr}_{1-x}\text{La}_x\text{FBiS}_2$ [16,18], and only small positive magnetoresistance due to the impurity phase Bi was reported in the $\text{Bi}_4\text{O}_4\text{S}_3$ system above T_c [29]. The magnetic-field dependence of magnetoresistance under several different tem-

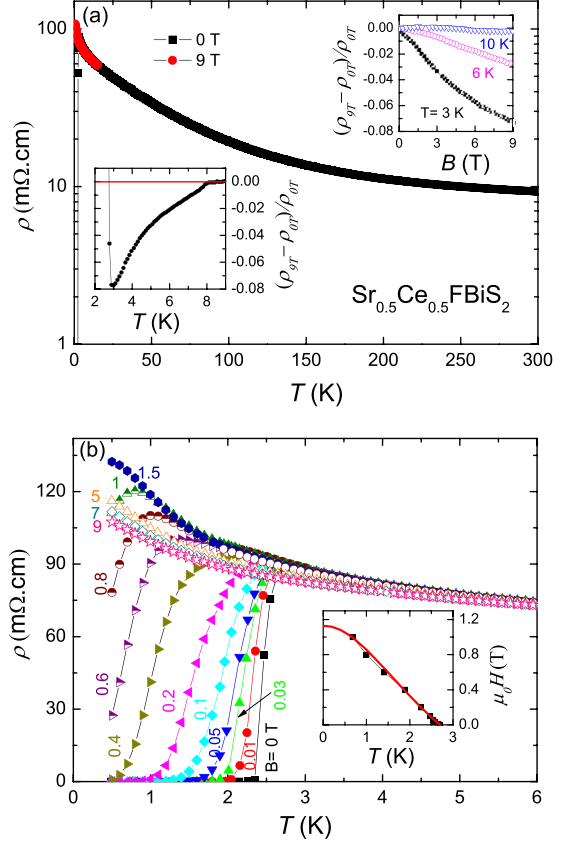


FIG. 2. (Color online) Temperature dependence of resistivity ρ for the $\text{Sr}_{0.5}\text{Ce}_{0.5}\text{FBiS}_2$ samples under zero field and 9 T. The upper inset shows the field dependence of magnetoresistance for the $\text{Sr}_{0.5}\text{Ce}_{0.5}\text{FBiS}_2$ sample under several fixed temperatures ($T = 3, 6, 10 \text{ K}$). The lower inset shows an enlarged plot of magnetoresistance around T_{FM} . (b) Temperature dependence of (magneto-) resistivity for $\text{Sr}_{0.5}\text{Ce}_{0.5}\text{FBiS}_2$ sample under several constant magnetic fields. The inset shows the $\mu_0 H_{c2}$ as a function of temperature.

peratures above T_c is plotted in the upper inset of Fig. 2(a). The negative magnetoresistance for $T = 3 \text{ K}$ is clearly observed and almost reaches -8% under $B = 9 \text{ T}$, decreases gradually, and then disappears with increasing temperature to 10 K. This feature can be tentatively attributed to the FM ordering of Ce^{3+} moments (to be shown below).

Figure 2(b) shows the enlarged low- T resistivity for the $\text{Sr}_{0.5}\text{Ce}_{0.5}\text{FBiS}_2$ sample under various magnetic fields below 6 K. With the application of magnetic fields, the superconducting transition becomes broadened and T_c decreases toward lower temperature. Superconductivity is suppressed down to 0.7 K by a magnetic field as low as 1 T and disappears at 1.5 T. Meanwhile, its resistivity displays a semiconducting-like feature. With further increasing the magnetic field to 9 T, the negative magnetoresistance is observed in the normal state, consistent with the magnetoresistivity data as shown in Fig. 2(a). The similar result is also observed in the $\text{EuFe}_2\text{As}_{2-x}\text{P}_x$ superconductor [8], which was reported to be a rare ferromagnetic superconductor. The inset of Fig. 2(b) displays the upper critical field $\mu_0 H_{c2}(T)$, determined by using the 90% normal-state resistivity criterion, as a function of temperature. The $\mu_0 H_{c2}$ - T diagram shows nearly linear

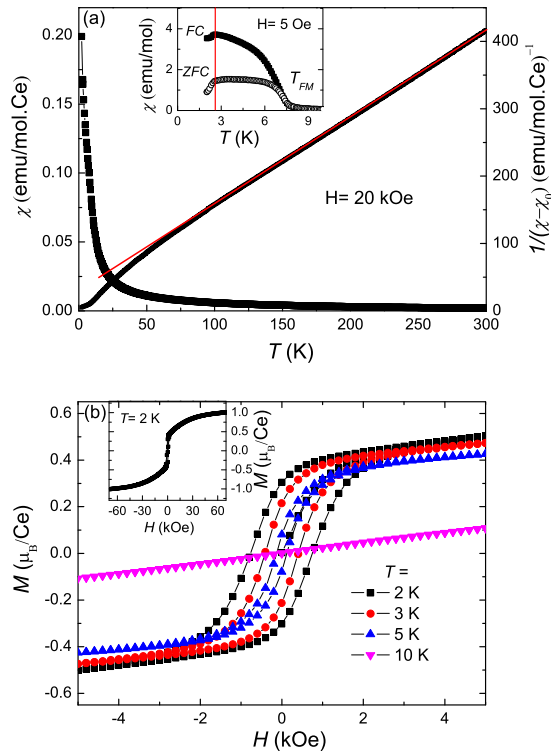


FIG. 3. (Color online) (a) Temperature dependence of magnetic susceptibility under $H = 20$ kOe for $\text{Sr}_{0.5}\text{Ce}_{0.5}\text{FBiS}_2$. The inset shows the ZFC (open symbols) and FC (solid symbols) susceptibilities under $H = 5$ Oe. (b) Isothermal magnetization of $\text{Sr}_{0.5}\text{Ce}_{0.5}\text{FBiS}_2$ sample at several different temperatures.

dependence in the measured temperature range. According to Ginzburg–Landau theory, the upper critical field H_{c2} evolves with temperature following the formula:

$$H_{c2}(T) = H_{c2}(0)(1 - t^2)/(1 + t^2), \quad (1)$$

where t is the renormalized temperature T/T_c . The upper critical field H_{c2} is estimated to be 1.16 T at $T = 0$ K, which is far smaller than that of Pauli paramagnetic limit $\mu_0 H_p = 1.84 T_c = 5$ T.

Figure 3(a) shows the temperature dependence of dc magnetic susceptibility for $\text{Sr}_{0.5}\text{Ce}_{0.5}\text{FBiS}_2$ under $B = 2$ T from 2 K to 300 K. The magnetic susceptibility above 100 K follows a modified Curie–Weiss behavior and can be fit to $\chi = \chi_0 + C/(T - \theta)$, where χ_0 denotes the temperature-independent term, C is the Curie–Weiss constant, and θ denotes the paramagnetic Curie temperature. By subtracting the temperature-independent term χ_0 , the $(\chi - \chi_0)^{-1}$ vs T , as plotted in Fig. 3(a), shows a linear behavior above 100 K. The fitting yields $C = 0.80$ emu K/mol Ce and $\theta = -19.2$ K. The effective magnetic moment μ_{eff} is thus calculated to be $2.53\mu_B$ per Ce, close to the theoretical value of $2.54\mu_B$ for a free Ce^{3+} ion.

To further investigate the coexistence of superconductivity and ferromagnetism in this sample, the magnetic susceptibility under 5 Oe with both zero-field-cooling (ZFC) and field-cooling (FC) modes below 10 K is depicted in the inset of Fig. 3(a). A rapid increase in the magnetic susceptibility and the obvious separation between ZFC and FC curves below

7.5 K may be ascribed to the long-range FM order of the Ce $4f$ ions, or the possible small ferromagnetic clusters [30]. With further cooling, an obvious drop around 2.8 K in both the ZFC and FC data is observed owing to the superconducting screening and Meissner effect, respectively. These results imply the coexistence of superconductivity and FM ordering in the system. Noted that the ZFC-FC hysteresis is slightly different to the case of a pure ferromagnetic system, suggesting a possibility for the existence of intercluster ferromagnetic interactions. The isothermal magnetization hysteresis loops for several temperatures are observed in Fig. 3(b). The clear hysteresis loop indicates a ferromagnetic-like order at 2 K on the sample. Moreover, the size of the loop gradually shrinks with increasing temperatures, and then disappears at 10 K. At higher magnetic fields for $T = 2$ K, the magnetization increases monotonically and then tends to saturate, as shown in the inset of Fig. 3(b). The largest saturated magnetic moment estimated is about $0.95\mu_B$, close to the $1\mu_B$ expected for a Ce^{3+} doublet ground state because of the crystal-field effect, similar to those of in $\text{CeFe}(\text{Ru})\text{PO}$ [31–33] and $\text{CeO}_{0.95}\text{F}_{0.05}\text{FeAs}_{1-x}\text{P}_x$ [9] compounds with ferromagnetic correlation [9,32]. It is worth noting that this hysteresis loop has not been reported thus far in other BiS_2 -based superconductors, even in the $\text{CeO}_{1-x}\text{F}_x\text{BiS}_2$ system [27].

The specific heat measurement of the $\text{Sr}_{0.5}\text{Ce}_{0.5}\text{FBiS}_2$ sample was plotted in Fig. 4. $C(T)$, in Fig. 4(a), shows a Dulong–Petit law and saturates to the classical limit of $3NR \sim 120 \text{ J K}^{-1} \text{ mol}^{-1}$ at high temperature, where N denotes the number of elements per formula unit. A clear λ -shaped kink at ~ 7.5 K is observed, strongly demonstrating the second-order phase transition. With increasing magnetic field, the anomaly shifts to higher temperature and becomes rather broadened, consistent with a FM nature of the transition, as shown in the lower inset of Fig. 4(a). Reminiscent of the features in the magnetic susceptibility and resistivity data around this temperature, the heat-capacity anomaly is ascribed to the ferromagnetic ordering of Ce moments. However, through subtracting the fit results from the raw data, a specific-heat anomaly associated with the superconducting transition is detected below T_c in the upper inset of Fig. 4(a). The jump, ΔC at T_c , is much weaker than that of the other BiS_2 -based superconductors [16], suggesting that the superconducting jump has been reduced by the magnetic signal. It has been reported that both $\text{CeO}_{0.5}\text{F}_{0.5}\text{BiS}_2$ and $\text{YbO}_{0.5}\text{F}_{0.5}\text{BiS}_2$ with magnetic rare-earth elements do not show any anomalies around T_c in the specific-heat data [34], while the clear jump is always observed in the systems with nonmagnetic elements, such as $\text{Sr}_{0.5}\text{La}_{0.5}\text{FBiS}_2$, $\text{LaO}_{1-x}\text{F}_x\text{OBiS}_2$ and $\text{La}_{1-x}\text{M}_x\text{OBiS}_2$ [16,35] whose normal state is paramagnetic. These results suggest that the anomaly around T_c may be overwhelmed by the enhanced specific-heat signal arising from the contribution of magnetic moments.

To further analyze the specific-heat data below 15 K, the specific heat can be written as $C = \gamma T + \beta T^3 + C_{\text{mag}} + C_{\text{sch}}$, where γ is the Sommerfeld coefficient, C_{mag} and $C_{\text{ph}} = \beta T^3$ represent the magnetic and phonon contributions, respectively, and C_{sch} is equal to α/T^2 , representing the Schottky anomaly item. We first fit the low- T specific heat below 3 K to obtain the Schottky anomaly item C_{sch} due to the contributions of nuclear spins. By subtracting the C_{sch} from the total specific heat, C/T

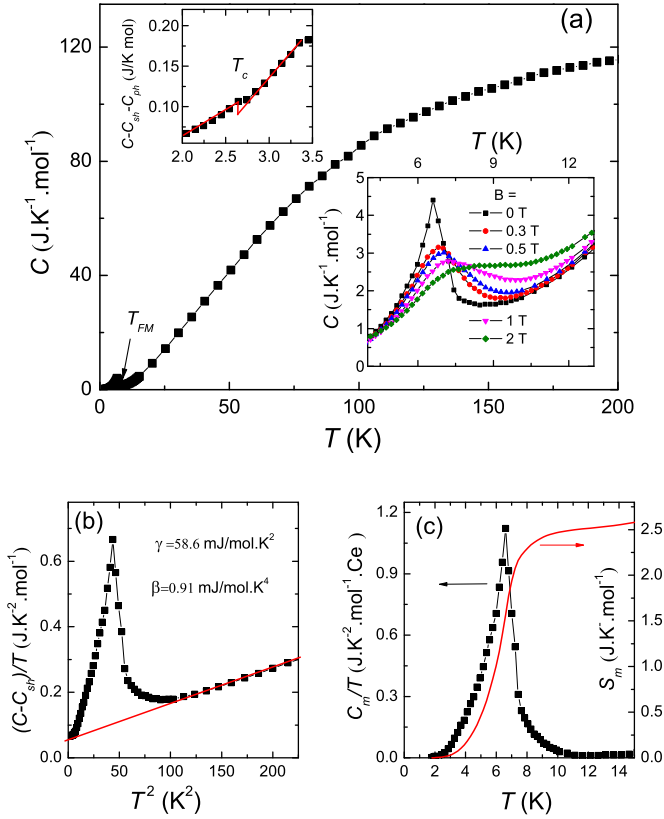


FIG. 4. (Color online) (a) Temperature dependence of specific heat for $\text{Sr}_{0.5}\text{Ce}_{0.5}\text{FBiS}_2$ under zero field below 200 K. The upper-left panel shows the specific-heat anomaly at 2.8 K because of the superconducting transition. The lower-right panel shows the magnetic specific-heat anomaly around 7.5 K under several magnetic fields. (b) C/T vs T^2 in the low- T region (the dashed line obeys $C/T = \gamma + \beta T^2$). (c) The temperature dependence of the C_m/T (where C_m denotes magnetic contribution to the specific heat) and entropy S_m .

versus T^2 shows a linear behavior from 10 to 15 K, yields values of $\gamma = 58.6 \text{ mJ mol}^{-1} \text{ K}^{-2}$ and the Debye temperature $\Theta = 220 \text{ K}$, as shown in the Fig. 4(b). This value falls in between those for $\text{CeO}_{0.5}\text{F}_{0.5}\text{BiS}_2$ (224 K) and $\text{YbO}_{0.5}\text{F}_{0.5}\text{BiS}_2$ (186 K) [34]. Considering that only 50% Ce are doped into the lattice, the γ value should be $117.2 \text{ mJ K}^{-2} \text{ mol}^{-1} \text{ Ce}^{-1}$ for the Ce end compound, which is enhanced by a factor of 50 to 80 compared with those of $\text{Sr}_{0.5}\text{La}_{0.5}\text{FBiS}_2$ ($1.42 \text{ mJ mol}^{-1} \text{ K}^{-2}$) [18] and $\text{La}_{1-x}\text{M}_x\text{OBiS}_2$ ($M = \text{Ti, Zr, Th}$; 0.58 to $2.21 \text{ mJ mol}^{-1} \text{ K}^{-2}$) [35]. The substantially enhanced γ may mainly originate from the electronic correlation effect from Ce $4f$ electrons. The magnetic contribution C_{mag} was

obtained by removing the contributions of electronic, C_{ph} and C_{sch} . The magnetic entropy estimated associated with the ferromagnetic ordering is $2.7 \text{ J K}^{-1} \text{ mol}^{-1} \text{ Ce}^{-1}$ around 10 K, which amounts to 50% of $R \ln(2J + 1)$ with $J = 1/2$ for Ce^{3+} ions below 15 K, as shown in the Fig. 4(c). Considered omission of magnetic entropy, the S_m value actually should be close to the limit of the Ce^{3+} . These results indicate that the superconductivity coexists with a bulk ferromagnetic-like order in the sample.

Thus far, a growing body of evidence for the coexistence of superconductivity and ferromagnetism has been reported. The vast majority of these systems show superconductivity before the ferromagnetic ordering and lead to the reentrant superconductivity overlapped with a magnetic phase, such as ErRh_4B_4 [36], $\text{ErNi}_2\text{B}_2\text{C}$ [37], and $\text{EuFe}_2\text{As}_{2-x}\text{P}_x$ [8]. In those systems, two separate sets of electrons may be responsible for magnetic ordering and superconductivity. In our case, however, the ferromagnetic transition temperature is substantially higher than T_c . The role of Ce doping is twofold: it provides carriers to BiS_2 layers inducing superconductivity and they ferromagnetically order in the $(\text{Sr,Ce})\text{F}$ sublattice. Compared with the previous reports [8,27], the remarkable feature here is that the FM ordering can be established in the diluted Ce lattice (50% Ce in the SrF layer) mainly due to the Ruderman–Kittel–Kasuya–Yosida interaction. More experiments (neutron and NMR) and theoretical insight may provide useful clues for this issue in BiS_2 -based superconductors.

IV. CONCLUSION

In summary, by partially substituting Ce for Sr in the newly discovered SrFBiS_2 system, a ferromagnetic-like bulk ordered phase was put in evidence for temperatures below 7.5 K by transport, specific heat, and dc-magnetization measurements. Interestingly, this magnetic phase due to Ce^{3+} order coexists with superconductivity as temperature is lowered below $T_c = 2.8 \text{ K}$. In this system, Ce substitution likely provides carriers to the superconducting BiS_2 layers and, at the same time, it induces a FM ordering in the blocking $(\text{Sr,Ce})\text{F}$ layers.

Note added. Recently, we became aware of the recent paper [38], which also observed SC in $\text{Sr}_{1-x}\text{Ln}_x\text{FBiS}_2$ ($\text{Ln} = \text{Ce, Pr, Nd, Sm}$) systems.

ACKNOWLEDGMENTS

Y.L. would like to thank Yongkang Luo for inspiring discussions. This work was supported by the National Basic Research Program of China (Grants No. 2011CBA00103 and No. 2014CB921203), NSFC (Grants No. U1332209, No. 11104053, No. 11474080, and No. 61376094)

[1] N. F. Berk and J. R. Schrieffer, *Phys. Rev. Lett.* **17**, 433 (1966).
 [2] N. D. Mathur, *Nature (London)* **394**, 39 (1998).
 [3] D. J. Scalapino, *Rev. Mod. Phys.* **84**, 1383 (2012).
 [4] Y. Kamihara, T. Watanabe, M. Hirano, and H. Hosono, *J. Am. Chem. Soc.* **130**, 3296 (2008).
 [5] M. S. Torikachvili, S. L. Budko, N. Ni, and P. C. Canfield, *Phys. Rev. Lett.* **101**, 057006 (2008).

[6] S. S. Saxena, P. Agarwal, K. Ahilan, F. M. Grosche, R. K. W. Haselwimmer, M. J. Steiner, E. Pugh, I. R. Walker, S. R. Julian, P. Monthoux, G. G. Lonzarich, A. Huxley, I. Sheikin, D. Braithwaite, and J. Flouquet, *Nature (London)* **406**, 587 (2000).
 [7] D. Aoki, A. Huxley, E. Ressouche, D. Braithwaite, J. Flouquet, J. Brison, E. Lhotel, and C. Paulsen, *Nature (London)* **413**, 613 (2001).

- [8] Z. Ren, Q. Tao, S. Jiang, C. Feng, C. Wang, J. Dai, G. Cao, and Z. Xu, *Phys. Rev. Lett.* **102**, 137002 (2009).
- [9] Y. K. Luo, H. Han, S. Jiang, X. Lin, Y. K. Li, J. H. Dai, G. H. Cao, and Z. A. Xu, *Phys. Rev. B* **83**, 054501 (2011).
- [10] Y. Mizuguchi, H. Fujihisa, Y. Gotoh, K. Suzuki, H. Usui, K. Kuroki, S. Demura, Y. Takano, H. Izawa, and O. Miura, *Phys. Rev. B* **86**, 220510(R) (2012).
- [11] Y. Mizuguchi, S. Demura, K. Deguchi, Y. Takano, H. Fujihisa, Y. Gotoh, H. Izawa, and O. Miura, *J. Phys. Soc. Jpn.* **81**, 114725 (2012).
- [12] S. Demura, Y. Mizuguchi, K. Deguchi, H. Okazaki, H. Hara, T. Watanabe, S. J. Denholme, M. Fujioka, T. Ozaki, H. Fujihisa, Y. Gotoh, O. Miura, T. Yamaguchi, H. Takeya, and Y. Takano, *J. Phys. Soc. Jpn.* **82**, 033708 (2013).
- [13] V. P. S. Awana, A. Kumar, R. Jha, S. Kumar, J. Kumar, and A. Pal, *Solid State Commun.* **157**, 21 (2013).
- [14] J. Xing, S. Li, X. Ding, H. Yang, and H. H. Wen, *Phys. Rev. B* **86**, 214518 (2012).
- [15] R. Jha, S. K. Singh, and V. P. S. Awana, *J. Supercond. Novel Magn.* **26**, 499 (2013).
- [16] X. Lin, X. X. Ni, B. Chen, X. F. Xu, X. X. Yang, J. H. Dai, Y. K. Li, X. J. Yang, Y. K. Luo, Q. Tao, G. H. Cao, and Z. A. Xu, *Phys. Rev. B* **87**, 020504 (2013).
- [17] H. C. Lei, K. F. Wang, M. Abeykoon, E. S. Bozin, and C. Petrovic, *Inorg. Chem. (Washington, DC, US)* **52**, 10685 (2013).
- [18] Y. K. Li, X. Lin, L. Li, N. Zhou, X. F. Xu, C. Cao, J. H. Dai, L. Zhang, Y. K. Luo, W. H. Jiao, Q. Tao, G. H. Cao, and Z. Xu, *Supercond. Sci. Technol.* **27**, 035009 (2014).
- [19] B. Li, Z. W. Xing, and G. Q. Huang, *arXiv:1210.1743*.
- [20] C. T. Wolowiec, B. D. White, I. Jeon, D. Yazici, K. Huang, and M. B. Maple, *J. Phys.: Condens. Matter* **25**, 422201 (2013).
- [21] Y. Liang, X. Wu, W. F. Tsai, and J. P. Hu, *Front. Phys.* **9**, 194 (2014).
- [22] T. Yildirim, *Phys. Rev. B* **87**, 020506(R) (2013).
- [23] G. B. Martins, A. Moreo, and E. Dagotto, *Phys. Rev. B* **87**, 081102(R) (2013).
- [24] G. Lamura, T. Shiroka, P. Bonfa, S. Sanna, R. De Renzi, C. Baines, H. Luetkens, J. Kajitani, Y. Mizuguchi, O. Miura, K. Deguchi, S. Demura, Y. Takano, and M. Putti, *Phys. Rev. B* **88**, 180509 (2013).
- [25] L. K. Zeng, X. B. Wang, J. Ma, P. Richard, S. M. Nie, H. M. Weng, N. L. Wang, Z. Wang, T. Qian, and H. Ding, *Phys. Rev. B* **90**, 054512 (2014).
- [26] Z. R. Ye, H. F. Yang, D. W. Shen, J. Jiang, X. H. Niu, D. L. Feng, Y. P. Du, X. G. Wan, J. Z. Liu, X. Y. Zhu, H. H. Wen, and M. H. Jiang, *Phys. Rev. B* **90**, 045116 (2014).
- [27] S. Demura, K. Deguchi, Y. Mizuguchi, K. Sato, R. Honjyo, A. Yamashita, T. Yamaki, H. Hara, T. Watanabe, S. J. Denholme, M. Fujioka, H. Okazaki, T. Ozaki, O. Miura, T. Yamaguchi, H. Takeya, and Y. Takano, *arXiv:1311.4267*.
- [28] B. Chen, C. Uher, L. Iordanidis, and M. G. Kanatzidis, *Chem. Mater.* **9**, 1655 (1997).
- [29] S. Li, H. Yang, J. Tao, X. Ding, and H. H. Wen, *Sci. China: Phys., Mech. Astron.* **56**, 2019 (2013).
- [30] R. P. Panmand, M. V. Kulkarni, M. Valant, S. W. Gosavi, and B. B. Kale, *AIP Adv.* **3**, 022123 (2013).
- [31] C. Krellner, N. S. Kini, E. M. Bruning, K. Koch, H. Rosner, M. Nicklas, M. Baenitz, and C. Geibel, *Phys. Rev. B* **76**, 104418 (2007).
- [32] E. M. Bruning, C. Krellner, M. Baenitz, A. Jesche, F. Steglich, and C. Geibel, *Phys. Rev. Lett.* **101**, 117206 (2008).
- [33] S. X. Chi, D. T. Adroja, T. Guidi, R. Bewley, S. L. Li, J. Zhao, J. W. Lynn, C. M. Brown, Y. Qiu, G. F. Chen, J. L. Lou, N. L. Wang, and P. C. Dai, *Phys. Rev. Lett.* **101**, 217002 (2008).
- [34] D. Yazici, K. Huang, B. D. White, A. H. Chang, A. J. Friedman, and M. B. Maple, *Philos. Mag.* **93**, 673 (2013).
- [35] D. Yazici, K. Huang, B. D. White, I. Jeon, V. W. Burnett, A. J. Friedman, I. K. Lum, M. Nallaiyan, S. Spagna, and M. B. Maple, *Phys. Rev. B* **87**, 174512 (2013).
- [36] W. A. Fertig, D. C. Johnston, L. E. DeLong, R. W. McCallum, M. B. Maple, and B. T. Matthias, *Phys. Rev. Lett.* **38**, 987 (1977).
- [37] P. C. Canfield, S. L. Bud'ko, and B. K. Cho, *Phys. C (Amsterdam, Neth.)* **262**, 249 (1996).
- [38] R. Jha, B. Tiwari, and V. P. S. Awana, *arXiv:1407.3105*.